Ethynylene-Bridged Pentacene Trimer and Tetramer Prepared Through Unexpected Oligomerization and Their Subsequent Thermal Conversions

Hironobu Hayashi,*[a,b] Juanjuan Zhu,[b] Naoto Minamino,[b] Yuya Murakami,[b] Shoma Kasahara,[c] Kyohei Matsuo,[b,c] Naoki Aratani,[b] Hiroko Yamada*[b,c]

Dedication ((optional))

[a] Dr. H. Hayashi
Center for Basic Research on Materials
National Institute for Materials Science (NIMS)
1-2-1 Sengen, Tsukuba, Ibaraki 305-0047 (Japan)
[b] Dr. H. Hayashi, Dr. J. Zhu, N. Minamino, Y. Murakami, Dr. K. Matsuo, Prof. Dr. N. Aratani, Prof. Dr. H. Yamada
Division of Materials Science
Nara Institute of Science and Technology (NAIST)
8916-5 Takayama-cho, Ikoma, Nara 630-0192 (Japan)
[c] S. Kasahara, Dr. K. Matsuo, Prof. Dr. H. Yamada
Institute for Chemical Research
Kyoto University
Gokasho, Uji, Kyoto 611-0011 (Japan)
E-mail: HAYASHI.Hironobu@nims.go.jp, hyamada@scl.kyoto-u.ac.jp

Supporting information for this article is given via a link at the end of the document.

Abstract: Ethynylene-bridged acenes, which are π-conjugated triple bond-containing systems, have attracted increasing interest as promising organic semiconductor materials due to their delocalized π-electrons. In this study, ethynylene-bridged pentacene precursor oligomers were not only synthesized through multiple-organic reactions but also were unexpectedly obtained in one-pot by using a conventional reaction with lithium silylacetylide and quinone. In the case of one-pot synthesis, the formation of oligomers, including pentamer, was evidently confirmed by matrix-assisted-laser-desorption/ionization time-of-flight mass spectrometry. Single crystal X-ray analysis visualized the ethynylene-bridged structure of the dimer which was one of the major products in the one-pot reaction. It was found that the reaction time for the lithiation was the key factor in controlling oligomer formation. Finally, the thermal conversion from pentacene precursors to the corresponding pentacene oligomers was achieved *via retro*-Diels–Alder reaction. These results would open an access to synthesize a wide range of π-conjugated systems.

Introduction

Silylethynylenes have been often introduced for organic semiconducting materials. It is well-known that the proper choice of silylethynylene has the potential to control the packing structure of small molecules, while also providing reasonable solubility to the molecules.[1–6] This aspect is quite attractive for solution-processed organic semiconducting devices. For example, 6,13-bis(triisopropylsilylethynyl)pentacene (**TIPSpen**), reported by Anthony in 2002, is the most famous acene derivatives with efficient charge transport property.[7] Subsequently, numerous researchers have synthesized **TIPSpen** and its derivatives by using a typical reaction with pentacenequinone (or suitable quinones) and lithium silylacetylide followed by the reductive aromatization. Concurrently, in terms of synthetic ease, the desilylation of silylethynylene substituted π-conjugated systems would be the preferable choice to generate oligoarylene ethynylene systems.[8–16] The desilylation followed by coupling reactions such as Sonogashira reactions could yield a wide range of valuable ethynylene-bridged acenes.

Ethynylene-bridged acenes, that is a π-conjugated triple-bond-containing system, have attracted increasing interest as promising organic semiconductor materials due to their delocalized π-electrons.[8–16] The easy modification of π-conjugation lengths by controlling the repeating unit of ethynylene-bridges allows the flexible demand in the application of electronic materials. For example, ethynylene-bridged anthracene oligomers exhibited specific hole mobility depending on the repeating units. The top-contact bottom-gate organic field-effect transistor (FET) devices of trimer exhibited better hole mobility (8.0×10^{-3} cm^2 V^{-1} s^{-1}) than dimer (8.9×10^{-4} cm^2 V^{-1} s^{-1}).[10] In addition, the single-crystal FET devices of trimer showed mobility up to 0.14 cm^2 V^{-1} s^{-1}, which was higher than that of tetramer. Importantly, these results suggested that the enhancement of two-dimensional electronic interaction in the system by π-expansion of core acene, from anthracene to pentacene, would be effective in improving the charge transport property. Considering that crystalline dip-coated films of ethynylene-bridged pentacene dimer exhibited the hole mobility of 0.24 cm^2 V^{-1} s^{-1},[15] improved charge transport property is highly expected for ethynylene-bridged pentacene trimer. In addition, recent studies indicated the importance of ethynylene-bridged acene systems not only as efficient semiconducting materials but also as topological materials by tuning their π-conjugation, because of transformations between two resonant structures.[17,18]

Although the π-expansion from anthracene to pentacene could provide insights into the preparation of efficient semiconducting and topological materials, the instability of pentacene presents significant synthetic challenges. A protection/deprotection method is often employed in the synthesis of ethynylene-bridged pentacene oligomers to avoid reactive nature of pentacenes.[19] On the other hand, we have demonstrated thermal precursor approaches to overcome these problems, such as the low solubility and instability of pentacene and polyacene derivatives.[20,21] Briefly, bicyclo[2.2.2]octadiene(BCOD)-fused acenes can be converted to the corresponding acenes by a thermally induced *retro*-Diels–Alder reaction (Figure 1). Importantly, the precursor molecules are often more soluble and stable than the corresponding ones. The thermal conversion could be performed at the final stage. There is no need to purify the resulting materials, if the precursor is pure enough, as the *retro*-Diels–Alder reaction produced only ethylene molecules as a gaseous byproduct.

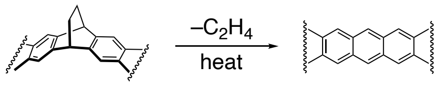

Figure 1. *retro*-Diels–Alder reaction of BCOD moiety.

In this study, the synthesis of a series of ethynylene-bridged pentacene trimer (**Pen3mer**) and tetramer (**Pen4mer**) was investigated by using precursor method (Figure 2). During the course of the synthesis, the precursors of the oligomers were found to be synthesized from BCOD-fused anthraquinone (**BCODquinone**) in one-pot, skipping several reaction steps. Finally, the conversion from precursors to the corresponding pentacene oligomers was achieved through *retro*-Diels–Alder reaction.

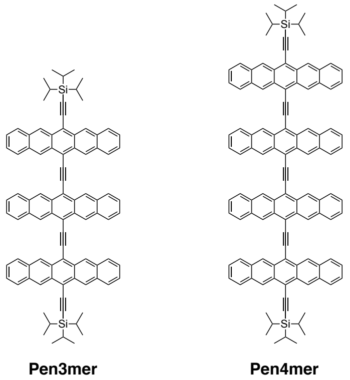

Figure 2. Ethynylene-bridged pentacene trimer and tetramer employed in this study.

Results and Discussion

Firstly, the ethynylene-bridged pentacene trimer precursor (**BCOD3mer**) was synthesized from **BCODquinone**[22] by using a conventional protection/deprotection method of silyl groups[19] as shown in Scheme 1. Here, compounds bearing BCOD groups are mixtures of stereoisomers regarding orientation of BCOD groups.[23] The key intermediate of compound **1** was prepared from **BCODquinone** and 1.2 equivalent of lithium TIPSacetylide (TIPSCCLi) in good yield (71%). Additionally, **BCOD1mer** was also successfully synthesized through a typical reaction with TIPSCCLi and **BCODquinone**, followed by the Sn^{II}-mediated reductive aromatization with 81% yield. After the deprotection of **BCOD1mer**, the addition of terminal ethynylenes-lithiated compound **2** to a tetrahydrofuran (THF) solution of compound **1**, followed by the Sn^{II}-mediated reductive aromatization, gave **BCOD3mer**. Note that the deprotection of silyl groups could be safely applied to **BCOD1mer** because it does not possess pentacene backbone, while **TIPSpen** is known to be decomposed easily after the desilylation.[19,24]

Interestingly, an unexpected oligomerization was observed during the preparation of **BCOD1mer** in Scheme 1, when the reaction was performed under slightly different reaction conditions (Scheme 2). The reaction afforded not only the expected monomer (**BCOD1mer**) but also unexpected oligomers, even up to pentamer (**BCOD5mer**) of the ethynylene-bridged pentacene precursor. Indeed, the formation of **BCOD2mer** was conceivable, as such a dimer formation with acenequinone and lithium silylacetylide has been already reported by Barlier[25] and our group.[15] These previous reports suggested that the reaction mechanism for the dimer formation was promoted by the deprotection of the silyl group, competing with the hydrolysis/reduction step in a kinetic process.

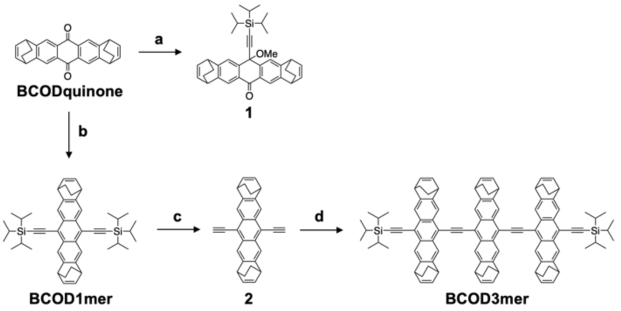

Scheme 1. Multi-step synthesis for **BCOD3mer**. Reaction conditions: a) 1) TIPSCCLi (1.2 eq), THF, 2) CH_3I, 71%; b) TIPSCCLi (10 eq), 2) $SnCl_2$, 10% H_2SO_4aq., 81%; c) tetrabutylammonium fluoride, THF, 72%, d) 1) *n*BuLi, THF, 2) compound **1**, 3) $SnCl_2$, 10% H_2SO_4aq., 16%.

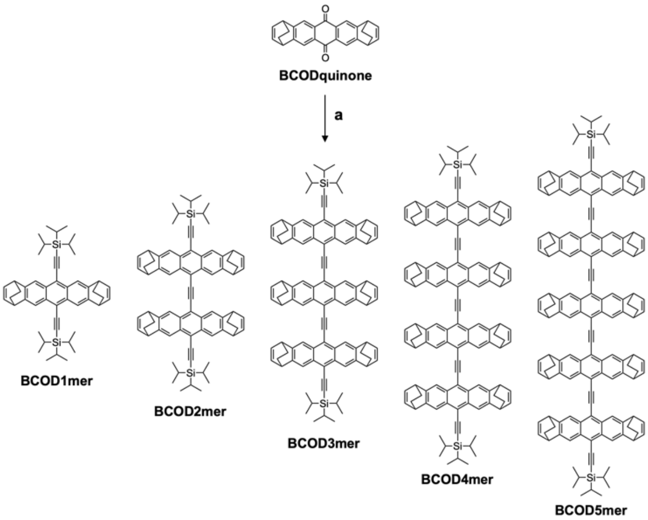

Scheme 2. One-pot synthesis of a series of ethynylene-bridged pentacene precursor oligomers. Reaction conditions: a) 1) TIPSCCLi, THF, 2) $SnCl_2$, 10% H_2SO_4aq. Yields of each oligomer depend on the reaction time for lithiation. See table 1 for the details.

By contrast with the previous reports on the dimer formation, matrix-assisted-laser-desorption/ionization time-of-flight mass spectrometry (MALDI-TOF-MS) of crude materials obtained from the reaction with **BCODquinone** and TIPSCCLi detected peaks of oligomers up to **BCOD5mer** (Figure 3). Indeed, high-resolution (HR) MALDI-TOF-MS evidently detected parent ion peaks at *m*/*z* = 694.4389 (calcd. for $C_{48}H_{62}Si_2$ = 694.4385 [M]$^+$) for **BCOD1mer**, at *m*/*z* = 1050.5952 (calcd. for $C_{76}H_{82}Si_2$ = 1050.5950 [M]$^+$) for **BCOD2mer**, at *m*/*z* = 1406.7520 (calcd. for $C_{104}H_{102}Si_2$ = 1406.7515 [M]$^+$) for **BCOD3mer**, at *m*/*z* = 1762.9077 (calcd. for $C_{132}H_{122}Si_2$ = 1762.9080 [M]$^+$) for **BCOD4mer**, and at *m*/*z* = 2119.0639 (calcd. for $C_{160}H_{142}Si_2$ = 2119.0645 [M]$^+$) for **BCOD5mer** (See Supporting Information). It was found that the reaction time for the lithiation of TIPSethynylene greatly affected the oligomer formation (Table 1). For example, 0.5-h-lithiation-time resulted in the oligomer formation with the yield of **BCOD1mer** (44%), **BCOD2mer** (23%), **BCOD3mer** (1%), **BCOD4mer** (0.3%), and **BCOD5mer** (trace), while longer lithiation times (4 h and 8 h) primarily yielded **BCOD1mer** with higher yields. The reaction yield again decreased after 12 h probably because of quenching of the generated TIPSCCLi. It should be noted that the acceptable yield of **BCOD2mer** through one-pot synthesis greatly reduced the need of laborious multi-step synthesis for preparing **BCOD2mer** (Scheme S1). In fact, **BCOD2mer** was used as an important building block for further oligomerization (*vide infra*). Additionally, the isolations of **BCOD3mer** and **BCOD4mer** were also achieved in spite of their low yields, while it was challenging to obtain sufficient amounts of **BCOD5mer**. The formation of these oligomers was further confirmed by ^{1}H NMR measurements and mass spectroscopy measurements (See Supporting Information). The bulky BCOD moieties in **BCODquinone** could be an important factors in this oligomerization in terms of the solubility. Even though the intermediate of this reaction possesses a stair-like conformation with much better solubility compared with the corresponding acene,[15] the solubility of the intermediate prepared from acene quinone without BCOD moieties would become lower with increasing the number of repeated acene units. Indeed, we confirmed that even anthraquinone could provide ethynylene-bridged anthracene trimer and tetramer by using the similar conditions, clearly demonstrating the generality of this oligomerization, although an enormous amount of anthraquinone (ca. 10 g) provided only a trace amount of the corresponding trimer and tetramer. So far, despite being a common strategy for synthesizing ethynylene-bridged acene oligomers, this specific oligomerization beyond dimers from acenequinone has not been previously reported.[15,25] The discovery in this study implies that the solubility of the intermediate may limit the further oligomerization. This unexpected oligomerization, which was hidden in a conventional reaction, provides a great clue to an effective synthetic approach of ethynylene-bridged compounds.

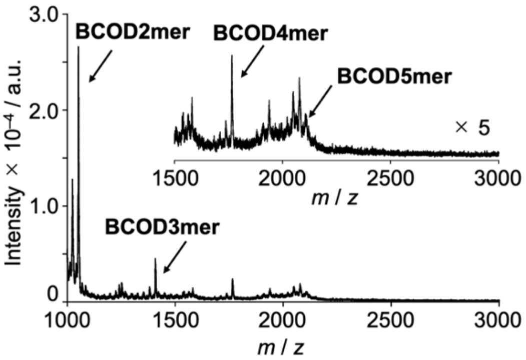

Figure 3. MALDI-TOF-MS spectrum of crude materials. **BCOD1mer** was removed before measurement to improve the peak intensities of other oligomers. Inset is magnified spectrum in the range from 1500 to 3000 *m*/*z*.

Table 1. Relationship between lithiation time and reaction yield of oligomers.

Lithiation time[a)]	Reaction yield [%]				
	BCOD1mer	BCOD2mer	BCOD3mer	BCOD4mer	BCOD5mer
0 h	34	25	trace	0	0
0.5 h	44	23	1	0.3	trace[b)]
4 h	71	15	0.5	0.3	trace[b)]
8 h	81	6	0.5	0.1	0
12 h	25	6	trace[b)]	0	0

[a)] Lithiation of TIPSethynylene. [b)] Confirmed only by mass spectroscopy.

Owing to the acceptable yield of **BCOD2mer** *via* one-step synthesis, **BCOD4mer** was successfully synthesized through two steps from **BCOD2mer** (Scheme 3). Even with BCOD moieties, the solubility of **BCOD4mer** is considerably low. Despite its low solubility and highly reactive nature, the dilithiated compound **3** still produced **BCOD4mer** in relatively low but acceptable yields (9%).[10] These results indicate that the further optimization for one-pot synthesis has the potential to use oligomers as key intermediates for extremely long ethynylene-bridged acene compounds.

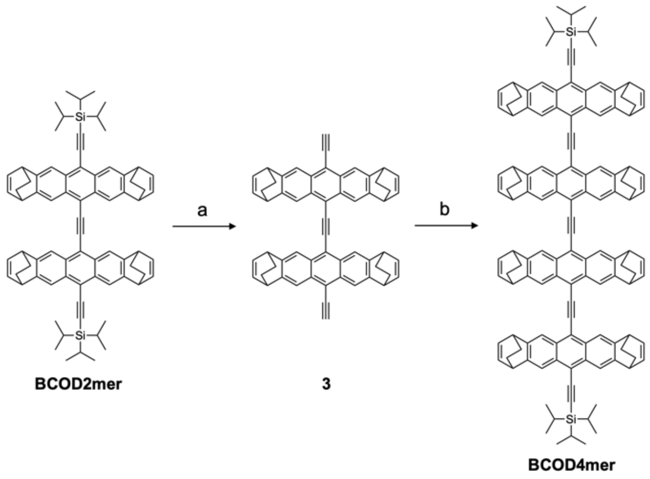

Scheme 3. Synthesis of **BCOD4mer**. Reaction conditions: a) tetrabutylammonium fluoride, THF, 98%, b) 1) *n*BuLi, THF, 2) compound **1**, 3) $SnCl_2$, 10% H_2SO_4aq., 9%.

The structures of **BCOD1mer**[26] and **BCOD2mer**[27] were unambiguously confirmed by single crystal X-ray analysis (Figure 4). The results clearly indicate that 1,4,8,11-tetrahydro-1,4:8,11-diethanopentacene (pentacene precursor moiety) is bridged through an ethynylene spacer in **BCOD2mer**. **BCOD1mer** possesses an almost planar π-system, and two pentacene precursor moieties in **BCOD2mer** show a near-coplanar arrangement (Figure 4a,b). The presence of the ethynylene spacer weakens the repulsion of the hydrogen atoms in adjacent pentacene precursor units, as seen in the case of ethynylene-bridged pentacene dimer.[10,15] In the crystal, each **BCOD2mer** molecule effectively interacts with four different neighboring molecules by CH-π interactions, forming a brickwork motif packing (Figure 4c). The bulky BCOD units resulted in a relatively large interplane distance of 4.7 Å between stacked pentacene precursor moieties, suggesting difficulty in efficient charge transport with this form. **BCOD3mer** also produced the crystals by using similar conditions, but the obtained stacked plate crystals were not suitable for single crystal X-ray analysis.

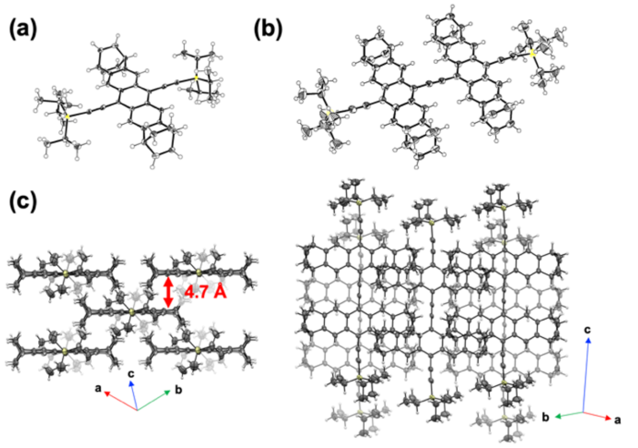

Figure 4. Single crystal X-ray structures of a) **BCOD1mer** and b) **BCOD2mer**. Packing structure of **BCOD2mer** is shown in (c). The thermal ellipsoids are shown at 50% probability.

Normalized UV-vis absorption spectra of oligomers in dichloromethane (DCM) are shown in Figure 5. The absorption bands at the longest wavelength red-shifted as the number of repeated units increased. The absorption maximum of **BCOD4mer** (λ_{max} = 575 nm) shifted to a longer wavelength (137 nm) compared with **BCOD1mer** (λ_{max} = 438 nm), indicating the effective π-elongation. The broadening absorption spectra with increasing degrees of oligomerization resemble those of ethynylene-bridged anthracene oligomers in the previous report.[10] This implies the relative energy differences between the molecular conformations with different torsional angles, and therefore the presence of the several conformations due to the rotation of the pentacene precursor units.[10,28,29] At the same time, **BCOD3mer** and **BCOD4mer** exhibited broad absorption spectra with several peaks, whereas the corresponding ethynylene-bridged anthracene trimer and tetramer without BCOD groups showed entirely featureless absorption spectra. This result implies that the bulky BCOD groups likely prevent the central anthracene units from rotating, leading to the observed differences in optical properties.[10] The fluorescence spectra followed a similar trend. The fluorescence maximum was red-shifted from 447 nm (**BCOD1mer**) to 628 nm (**BCOD4mer**) with Stokes shifts of 0.057 eV (**BCOD1mer**) to 0.18 eV (**BCOD4mer**) (Table 2). In addition, the oligomers showed weaker fluorescence quantum yield Φ_f and shorter fluorescence lifetimes (Figure S1, Table S1) compared with **BCDO1mer** as the degree of oligomerization increased, indicating that the presence of ethynylene units facilitates quenching via nonradiative pathways as seen in ethynylene-bridged anthracene oligomers (Table S2).[10,30]

Cyclic voltammetry was carried out to investigate the electronic properties of oligomers in DCM using 0.10 M nBu$_4$NPF$_6$ as a supporting electrolyte (Figure S2). All redox potentials are given versus the ferrocene/ferrocenium (Fc/Fc$^+$) couple. Similar to their counterparts without BCOD units[10], the redox potentials varied significantly with an increase in anthracene units (Table S3). The oligomers with more anthracene units were more susceptible to oxidation, and the reduction potentials showed a similar trend, narrowing HOMO–LUMO gaps upon chain elongation. The trend of electrochemically determined HOMO–LUMO gaps are consistent with the optically estimated values.

Table 2. Summary of optical properties of oligomers in DCM.

	λ_{max} [a] [nm]	λ_{em} [b] [nm]	Φ_f [c] [%]	Stokes shift [eV]	τ [d] [ns]
BCOD 1mer	438	447	91	0.057	5.0
BCOD 2mer	520	541	54	0.092	2.8
BCOD 3mer	568	595	16	0.099	< 1
BCOD 4mer	575	628	5	0.18	< 1

[a]The longest absorption peaks; [b]Excited at 390 nm for **BCOD1mer**, 487 nm for **BCOD2mer**, 527 nm for **BOCD3mer**, and 536 nm for **BCOD4mer**; [c]Absolute fluorescence quantum yields. Excited wavelength is the same with the fluorescence measurement; [d]Excited at 405 nm.

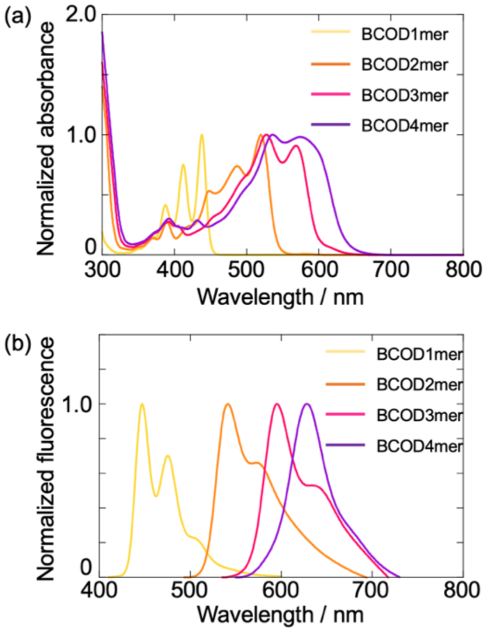

Figure 5. (a) Normalized absorption and (b) fluorescence spectra of oligomers in DCM. The solution was excited at 390 nm for **BCOD1mer**, 487 nm for **BCOD2mer**, 527 nm for **BOCD3mer**, and 536 nm for **BCOD4mer**.

Finally, the pentacene precursor oligomers were converted to the corresponding pentacene oligomers *via* heating in the solid state. Prior to the conversion, thermogravimetric analysis (TGA) was performed to investigate the reaction temperature. The TGA traces for **BCOD3mer** and **BCOD4mer** are shown in Figure 6. Stepwise eliminations of ethylene molecules *via retro*-Diels–Alder reaction were observed for **BCOD3mer**. The conversion of **BCOD3mer** started around 250 °C, and was completed when the temperature reached approximately 350–400 °C. The theoretical weight loss for six ethylene molecules (12%) was in good agreement with the experimental values (12% weight loss at 380 °C). In the case of **BCOD4mer**, the *retro*-Diels–Alder reaction proceeded all at once. The experimental weight loss of 12% at 340 °C is also in good agreement with the theoretical value (12.7%).

With these results in mind, the bulk powders of **BCOD3mer** and **BCOD4mer** were heated at 350 °C (for **BCOD3mer**) and 280 °C (for **BCOD4mer**) for 2 h under vacuum conditions. HR-MALDI-TOF-MS of the annealed solids evidently showed parent ion peaks at *m*/*z* = 1238.5629 (calcd. for $C_{92}H_{78}Si_2$ = 1238.5637 [M]$^+$) for **Pen3mer** (Figure S23) and *m*/*z* = 1538.6570 (calcd. for $C_{116}H_{90}Si_2$ = 1538.6576 [M]$^+$) for **Pen4mer** (Figure S24), supporting the conversion from precursor to ethynylene-bridged pentacene oligomers. After solid state conversion, the obtained powders containing **Pen3mer** and **Pen4mer** were quite insoluble in any media, and therefore the ^{1}H NMR measurement was difficult. Considering the poor solubility of ethynylene-bridged pentacene dimer in the previous report,[14] this feature is reasonable. The introduction of several substituents to acene backbone is worth considering to improve the solubility.[31]

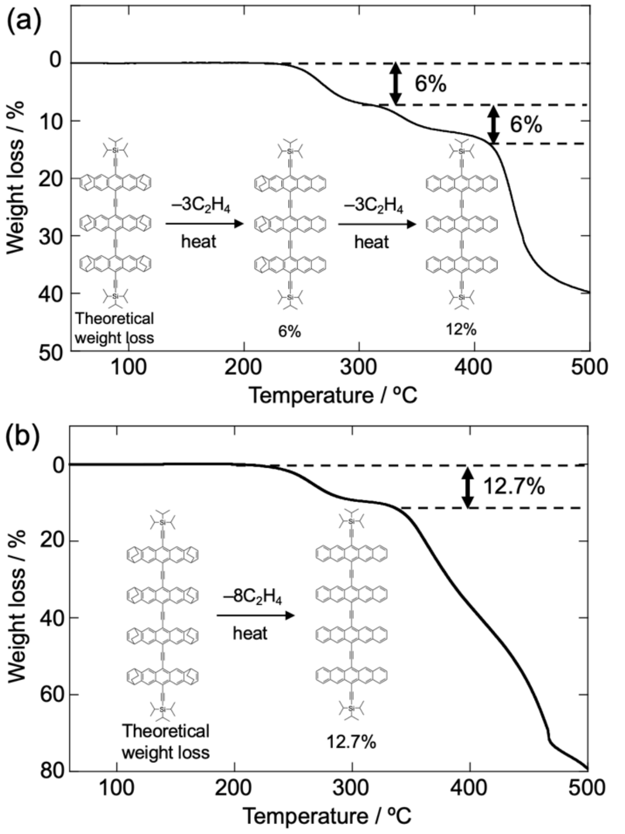

Figure 6. TGA analysis of (a) **BCOD3mer** and (b) **BCOD4mer** under N_2 atmosphere. Rate: 10 °C/min. Structural changes (only representative isomer) according to annealing is also shown.

The changes in optical properties were also investigated to evaluate the thermal conversion in liquid phase. The solution of **BCOD3mer** or **BCOD4mer** in diphenyl ether was subjected to high temperatures *via* microwave irradiations under N_2 atmosphere. After numerous attempts, it was discovered that **BCOD3mer** converted to **Pen3mer** through *retro*-Diels-Alder reactions by heating the diphenyl ether solution at 300 °C. Additionally, heating at 260–280 °C led to the conversion of **BCOD4mer** to **Pen4mer**. MALDI-TOF-MS spectra of the crude solution also showed the parent ion peaks of **Pen3mer** and **Pen4mer**, supporting their formations. The maximum absorption wavelengths of **Pen3mer** and **Pen4mer** were found to be approximately 770–800 nm (Figure 7). Note that broad and small shoulders were also observed at wavelengths exceeding 800 nm, which are also consistent with the absorption characteristics of diethynylene-bridged pentacene trimer and tetramer.[19] **Pen4mer** exhibited a slightly red-shifted absorption compared to **Pen3mer**, although their peak maxima were nearly identical. This implies that the effective π-conjugation length for this series of oligomers is essentially achieved at the stage of **Pen4mer**. Here, short-term heating (less than 10 minutes) proved to be more favorable than prolonged heating. When measuring the absorption spectra, a blue shift was observed with extended heating (ca. 30 minutes) compared to short-term heating. Even minor differences in heating duration and temperature resulted in variations in peak intensity, particularly in the 500–700 nm range of the absorption spectrum. This result might suggest the progression of the [4+2] reaction between the formed **Pen3mer** (or **Pen4mer**) molecules. However, it should be noted that the high temperature required also lead to undesirable decomposition of the products. Consequently, it is not clear that the blue-shifted peaks after extended heating conclusively prove the progression of the [4+2] reaction. Further optimization of reaction conditions is necessary to avoid side reactions and ensure the successful formation of **Pen3mer** and **Pen4mer**.

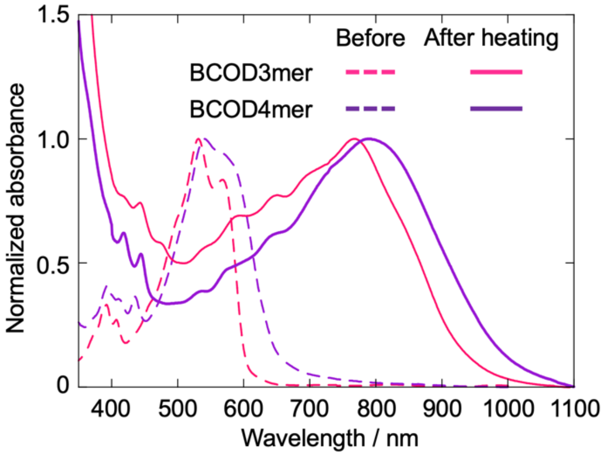

Figure 7. Representative normalized absorption spectra of **BCOD3mer** and **BCOD4mer** before (dashed line) and after (solid line) heating in diphenyl ether. Heating conditions: 300 °C, 3 minutes for **BCOD3mer**, and 260 °C, 5 minutes and then 280 °C, 90 seconds for **BCOD4mer** under N_2 atmosphere.

Conclusion

In summary, we have successfully synthesized ethynylene-bridged pentacene precursor oligomers through the conventional protection/deprotection method of silyl groups. During the course of the synthesis, unexpected oligomerization was discovered, producing oligomers up to a pentamer. The dimer formation with a relatively good yield in one-pot reaction enables us to synthesize a tetramer, skipping the laborious multi-step synthesis. The optical features of these oligomers reflect the effective π-conjugation as the numbers of acene units increase. Finally, the thermal conversion of precursors was attempted in both the solid state and liquid phase. TGA profiles and HR-MALDI-TOF-MS spectra of annealed powders of **BCOD3mer** and **BCOD4mer** suggested the formation of the corresponding ethynylene-bridged pentacene oligomers. In diphenyl ether, **BCOD3mer** and **BCOD4mer** were converted to **Pen3mer** and **Pen4mer**, respectively, by heating the solution to a high temperature. The maximum absorption wavelengths of **Pen3mer** and **Pen4mer** reached approximately 800 nm, supporting the oligomer formation with pentacene units. Additionally, it was found that their peak maxima were nearly identical, implying that the effective π-conjugation length for this series of oligomers is essentially achieved at the stage of **Pen4mer**. Further optimization of conversion reactions including the utilization of interior of single crystal[32] or metal organic framework[33], as well as detail characterization of oligomers, would lead to investigate the effect of π-elongation on hole mobility of ethynylene-bridged acene oligomers. We believe that this approach could potentially access a wide range of ethynylene-bridged acenes.

Supporting information

Deposition Numbers 2255619 (for **BCOD1mer**) and 2255620 (for **BCOD2mer**) contain the supplementary crystallographic data for this paper. These data are provided free of charge by the joint Cambridge Crystallographic Data Centre. An additional reference cited within the Supporting Information.[34]

Acknowledgements

We would like to thank Ms. Y. Nishikawa and Ms. M. Yamagaki for the mass spectrometry measurements. This work is partly supported by JST PRESTO (No. JPMJPR21AC), Grants-in-Aid for Scientific Research (Nos. JP20H02816, JP20H00379, JP20H05833, JP20H02711, JP22K19067, JP22K05255, and JP24K01576), and Masuyakinen basic research foundation. The authors also thank Mr. K. Kawano for fruitful discussion about oligomer synthesis.

Keywords: pentacene • oligomer • thermal conversion • single crystal • precursor approach

Reference

1. K. Takahashi, B. Shan, X. Xu, S. Yang, T. Koganezawa, D. Kuzuhara, N. Aratani, M. Suzuki, Q. Miao, H. Yamada, *ACS Appl. Mater. Interfaces*, **2017**, *9*, 8211–8218.
2. J. Zhu, H. Hayashi, M. Chen, C. Xiao, K. Matsuo, N. Aratani, L. Zhang, H. Yamada, *J. Mater. Chem. C*, **2022**, *10*, 2527–2531.
3. L. Zhang, A. Fonari, Y. Liu, A. L. M. Hoyt, H. Lee, D. Granger, S. Parkin, T. P. Russell, J. E. Anthony, J. L. Brédas, V. Coropceanu, A. L. Briseno, *J. Am. Chem. Soc.*, **2014**, *136*, 9248–9251.
4. J. E. Anthony, D. L. Eaton, S. R. Parkin, *Org. Lett.*, **2002**, *4*, 15–18.
5. J. Chen, S. Subramanian, S. R. Parkin, M. Siegler, K. Gallup, C. Haughn, D. C. Martin, J. E. Anthony, *J. Mater. Chem.*, **2008**, *18*, 1961–1969.
6. W. Chen, F. Yu, G. Zhou, Q. Zhang, *Adv. Sci.*, **2020**, *7*, 1903766.
7. J. E. Anthony, J. S. Brooks, D. L. Eaton, S. R. Parkin, *J. Am. Chem. Soc.*, **2001**, *123*, 9482–9483.
8. G. Romanazzi, A. Dell’Aquila, G. P. Suranna, F. Marinelli, S. Cotrone, D. Altamura, C. Giannini, L. Torsi, P. Mastrorilli, *J. Mater. Chem.*, **2011**, *21*, 15186–15189.
9. Keg, P., Dell’Aquila, A., Marinelli, F., Kapitanchuk, O. L., Fichou, D., Mastrorilli, P., Romanazzi, G., Suranna, G. P., Torsi, L., Lam, Y. M., Mhaisalkar, S. G. *J. Mater. Chem.*, **2010**, *20*, 2448–2456.
10. J. Zhu, H. Hayashi, M. Chen, C. Xiao, K. Matsuo, N. Aratani, L. Zhang, H. Yamada, *Macromol. Chem. Phys.*, **2021**, *222*, 2100024.
11. D. G. Whitten, Y. Tang, Z. Zhou, J. Yang, Y. Wang, E. H. Hill, H. C. Pappas, P. L. Donabedian, E. Y. Chi, *Langmuir*, **2019**, *35*, 307–325.
12. X. Zhao, C. Huang, M. Gulcur, A. S. Batsanov, M. Baghernejad, W. Hong, M. R. Bryce, and T. Wandlowski, *Chem. Mater.*, **2013**, *25*, 4340–4347.
13. L. J. O’Driscoll, M. R. Bryce, *Nanoscale*, **2021**, *13*, 10668–10711.
14. A. Broggi, I. Tomasi, L. Bianchi, A. Marrocchi, L. Vaccaro, *ChemPlusChem*, ***2014***, *79*, 486–507.
15. K. Kawano, H. Hayashi, S. Yoshimoto, N. Aratani, M. Suzuki, J. Yoshinobu, H. Yamada, *Chem. Eur. J*, **2018**, *24*, 14916–14920.
16. T. Okamoto, Z. Bao, *J. Am. Chem. Soc.*, **2007**, *129*, 10308–10309.
17. B. Cirera, A. Sánchez-Grande, B. de la Torre, J. Santos, S. Edalatmanesh, E. Rodríguez-Sánchez, K. Lauwaet, B. Mallada, R. Zbořil, R. Miranda, O. Gröning, P. Jelínek, N. Martín, D. Ecija, *Nat. Nanotechnol.*, **2020**, *15*, 437–443.
18. A. Sánchez-Grande, B. de la Torre, J. Santos, B. Cirera, K. Lauwaet, T. Chutora, S. Edalatmanesh, P. Mutombo, J. Rosen, R. Zbořil, R. Miranda, J. Björk, P. Jelínek, N. Martín, D. Écija, *Angew. Chem. Int. Ed.*, **2019**, *131*, 6559–6563.
19. D. Lehnherr, A. H. Murray, R. McDonald, R. R. Tykwinski, *Angew. Chem. Int. Ed.*, **2010**, *49*, 6190–6194.
20. H. Yamada, T. Okujima, N. Ono, *Chem. Commun.*, **2008**, 2957–2974.
21. H. Yamada, D. Kuzuhara, M. Suzuki, H. Hayashi, N. Aratani, *Bull. Chem. Soc. Jpn.*, **2020**, *93*, 1234–1267.
22. K. Tanaka, N. Aratani, D. Kuzuhara, S. Sakamoto, T. Okujima, N. Ono, H. Uno, H. Yamada, *RSC Adv.*, **2013**, *3*, 15310–15315.
23. Y. S. Chan, H. Hayashi, S. Sato, S. Kasahara, K. Matsuo, N. Aratani, H. Yamada, *Eur. J. Org. Chem.*, **2022**, e202200621.
24. D. Lehnherr, R. McDonald, R. R. Tykwinski, *Org. Lett.*, **2008**, *10*, 4163–4166.
25. V. S. Barlier, C. W. Schlenker, S. W. Chin, M. E. Thompson, *Chem. Commun.*, **2011**, *47*, 3754–3756.
26. Crystallographic data for **BCOD1mer**: $C_{48}H_{62}Si_2$, $M_w = 695.15$, Monoclinic, space group $P2_1/c$, $a = 8.774(5)$, $b = 19.423(11)$, $c = 12.281(7)$ Å, $\beta = 92.734(12)°$, $V = 2091(2)$ Å^3, $T = 90$ K, $Z = 2$, reflections measured 9706, 3081 unique. The final R_1 was 0.1051 ($I > 2\sigma(I)$), and the final wR on F^2 was 0.3001 (all data), GOF = 1.100.

27. Crystallographic data for **BCOD2mer**: $C_{76}H_{82}Si_2$, M_w = 1051.65, Triclinic, space group *P*-1, a = 9.1058(6), b = 9.1619(6), c = 21.9819(15) Å, α = 94.236(7)°, β = 90.579(6)°, γ = 115.379(8)°, V = 1650.6(2) Å^3, T = 103 K, Z = 1, reflections measured 22404, 6008 unique. The final R_1 was 0.0930 ($I > 2\sigma(I)$), and the final wR on F^2 was 0.2912 (all data), GOF = 1.067.
28. B. Eichler, J. Erickson, J. Keppen, A. Sykes, G. Sereda, *Tetrahedron Lett.*, **2015**, *56*, 4574–4577.
29. O. L. Kapitanchuk, *Mol. Cryst. Liq. Cryst.*, **2016**, *639*, 55–63.
30. M. Nagaoka, E. Tsurumaki, M. Nishiuchi, T. Iwanaga, S. Toyota, *J. Org. Chem.*, **2018**, *83*, 5784–5790.
31. W. Chen, X. Li, G. Long, Y. Li, R. Ganguly, M. Zhang, N. Aratani, H. Yamada, M. Liu, Q. Zhang, *Angew. Chem. Int. Ed.*, **2018**, *57*, 13555–13559.
32. H. Hayashi, N. Hieda, M. Yamauchi, Y. S. Chan, N. Aratani, S. Matsuo, H. Yamada, *Chem. Eur. J.*, **2020**, *26*, 15079–15083.
33. T. Kitao, T. Miura, R. Nakayama, Y. Tsutsui, Y. S. Chan, H. Hayashi, H. Yamada, S. Seki, T. Hitosugi, T. Uemura, *Nat. Synth.*, **2023**, *2*, 848–854.
34. K. Tanaka, N. Aratani, D. Kuzuhara, S. Sakamoto, T. Okujima, N. Ono, H. Uno, H. Yamada, *RSC Adv.*, **2013**, *3*, 15310–15315.